Environmental Science & Technology

pubs.acs.org/est

Article

RNA Hydrolysis at Mineral–Water Interfaces

Ke Zhang, Kun-Pu Ho, Anamika Chatterjee, Grace Park, Zhiyao Li, Jeffrey G. Catalano, and Kimberly M. Parker*

Cite This: *Environ. Sci. Technol.* 2023, 57, 8280–8288

Read Online

ACCESS | Metrics & More | Article Recommendations | Supporting Information

ABSTRACT: As an essential biomolecule for life, RNA is ubiquitous across environmental systems where it plays a central role in biogeochemical processes and emerging technologies. The persistence of RNA in soils and sediments is thought to be limited by enzymatic or microbial degradation, which occurs on timescales that are orders of magnitude faster than known abiotic pathways. Herein, we unveil a previously unreported abiotic pathway by which RNA rapidly hydrolyzes on the timescale of hours upon adsorption to iron (oxyhydr)oxide minerals such as goethite (α-FeOOH). The hydrolysis products were consistent with iron present in the minerals acting as a Lewis acid to accelerate sequence-independent hydrolysis of phosphodiester bonds comprising the RNA backbone. In contrast to acid- or base-catalyzed RNA hydrolysis in solution, mineral-catalyzed hydrolysis was fastest at circumneutral pH, which allowed for both sufficient RNA adsorption and hydroxide concentration. In addition to goethite, we observed that RNA hydrolysis was also catalyzed by hematite (α-Fe_2O_3) but not by aluminum-containing minerals (e.g., montmorillonite). Given the extensive adsorption of nucleic acids to environmental surfaces, we anticipate previously overlooked mineral-catalyzed hydrolysis of RNA may be prevalent particularly in iron-rich soils and sediments, which must be considered across biogeochemical applications of nucleic acid analysis in environmental systems.

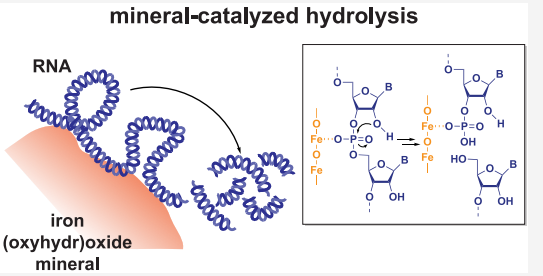

KEYWORDS: *abiotic RNA hydrolysis, mineral-catalyzed hydrolysis, surface-catalyzed hydrolysis, Lewis acid catalysis, phosphodiester bond cleavage*

INTRODUCTION

The environmental degradation of DNA has been widely studied due to its broad range of applications, including the measurement of environmental DNA in ecological surveys,[1−3] the prevalence of antibiotic resistance genes in the environment,[4] the detection of ancient genetic elements in archeology (i.e., ancient DNA),[5] and the elemental cycling of organic phosphorous.[6] The extensive adsorption of DNA to minerals in soils and sediments[7] has been consistently demonstrated to dramatically increase the persistence of DNA across numerous studies over decades of research.[7−14] For example, to achieve the same extent of enzymatic degradation as dissolved DNA, adsorbed DNA required incubation with orders of magnitude higher nuclease concentrations[10,12] and, in some cases, was permanently retained over the experiment duration.[9] The persistence of adsorbed DNA in environmental systems has largely been attributed to the reduced ability of nucleases in the environment to interact with DNA.[13,15] This protective effect of adsorption has been widely invoked to explain DNA persistence in the environment across disciplines.[1−5]

In recent years, RNA persistence in the environment has also gained increasing interest due to its relevance to an array of emerging applications. Environmental RNA has been used to analyze gene expression of microbial communities and improve resolution of biological monitoring.[1,16] The persistence of viral RNA has also been employed to quantify the abundance of pathogenic viruses including SARS-CoV-2 in water and wastewater systems (i.e., for wastewater-based epidemiology).[17−19] Noncoding RNA has also emerged in environmental contexts due to its potential role in cross-species interactions in soils[20,21] as well as its development as a pesticidal agent for use in agriculture,[22,23] where its persistence in receiving environments may result in increased risk to nontarget species.[24] Due to its high abundance in cells, released RNA may also contribute to biogeochemical processes (i.e., phosphorous cycling) in some environmental systems.[1]

In contrast to DNA, the presence of the 2′-hydroxyl group on the RNA structure reduces its chemical stability by facilitating hydrolysis of the phosphodiester backbone.[25,26] The 2′-hydroxyl group specifically enables an intramolecular nucleophilic attack on the phosphorous atom, leading to cleavage of the phosphodiester bond. This reaction is accelerated under certain solution conditions: deprotonation of the 2′-hydroxyl group under alkaline conditions increases its

Received: February 20, 2023
Revised: May 5, 2023
Accepted: May 8, 2023
Published: May 22, 2023

nucleophilicity,[25,26] while metals that act as Lewis acids can increase the electrophilicity of the phosphorous atom.[27−29] However, despite this structural instability, solution-phase abiotic RNA hydrolysis catalyzed by either hydroxide or metal ions has been found to be too slow to contribute to RNA degradation on relevant timescales (i.e., days) in environmental systems. Abiotic hydrolysis is further hindered for double-stranded (ds)RNA relative to single-stranded (ss)-RNA.[25,27] Consequently, degradation of dissolved RNA in environmental samples,[30,31] including those that have been sterilized to reduce microbial activity,[32] is likely attributable to hydrolysis by microbial nucleases, which are known to resist thermoinactivation.[33] Like DNA, RNA has been observed to strongly adsorb to minerals (e.g., iron (oxyhydr)oxides)[34] and to undergo rapid and extensive adsorption to particles in soils.[31,35] Analogous to DNA, RNA adsorbed to a synthetic clay nanoparticle was established to be protected from nucleases.[22] However, in apparent contradiction to the well-established protective effect of adsorption, RNA adsorbed to particles in soil undergoes rapid degradation, in some cases exceeding rates of solution-phase degradation in the same sample.[31,35] Specific processes that may contribute to RNA degradation upon adsorption to particles in environmental systems are yet to be identified.

We hypothesized that the apparent instability of adsorbed RNA may be attributable to the hydrolysis of phosphodiester bonds occurring at mineral−water interfaces. Notably, RNA hydrolysis is established to be catalyzed by dissolved metal ions acting as Lewis acids,[27,29] albeit at concentrations far higher than those encountered in environmental systems.[27] However, metals in certain minerals (i.e., iron (oxyhydr)oxides such as goethite) that are ubiquitous in soils and sediments may facilitate an analogous reaction for RNA adsorbed on mineral surfaces. Consequently, herein, we investigated the potential for mineral-catalyzed hydrolysis to contribute to rapid degradation of adsorbed RNA molecules in the environment.

MATERIALS AND METHODS

Chemicals and Supplies. All chemicals and supplies used in this study are detailed in Section S1. Nucleic acids (i.e., 1023 base pair (bp) DNA, 1000 bp double-stranded (ds)RNA, 1006 nucleotide (nt) single-stranded (ss)RNA, 106 nt ssRNA; sequences provided in Section S2) were synthesized using prior protocols employing polymerase chain reaction (PCR) for DNA synthesis and in vitro T7 polymerase for RNA synthesis.[25,35] We modified the final step of the DNA synthesis protocol so that the DNA product was eluted in molecular biology grade water to avoid experimental interference arising from constituents in the prior elution buffer (i.e., 10 mM tris(hydroxymethyl)aminomethane hydrochloride [Tris], pH 8.5).

Goethite, aluminum oxide, and silica were used directly as obtained from commercial sources (Section S3). Montmorillonite and kaolinite from the Clay Minerals Society's Source Clays Repository were pretreated to remove carbonate and retain fractions smaller than 2 μm (Section S3). Hematite and gibbsite were synthesized (Section S3). Minerals were analyzed to determine the surface area, point of zero charge, and (if synthesized) crystal structure. (Section S3).

We minimized the unintentional presence of RNase in our experiments using a prior protocol.[25] Specifically, we used RNase-free disposable supplies (e.g., tubes and pipettor tips), baked glassware (450 °C, 4 h), or reusable plasticware treated with 0.1% diethylpyrocarbonate (DEPC) for 8 h, followed by autoclaving to decompose DEPC. Buffers were prepared with ultrapure water, autoclaved, and aliquoted before storage at 4 °C (for <1 week) or at −20 °C (for long-term storage). All synthesis and experimental steps involving RNA prior to analysis were carried out in a laminar hood. Among materials used in this study, only minerals and organic matter (i.e., Suwannee River natural organic matter) were neither DEPC-treated nor autoclaved to avoid potential alterations to their chemical structures. However, all preparatory and pre-treatment steps for these materials exclusively used treated solutions and supplies. Organic matter solutions were additionally filtered through 0.22 μm membrane filters to remove particles and microbes. Because the addition of organic matter solutions suppressed rather than enhanced RNA hydrolysis on mineral surfaces as detailed below, the contribution of RNases in organic matter to RNA hydrolysis was inferred to be insignificant in our experiments. Specific efforts to quantify residual RNase activity in mineral-containing samples were not performed because available protocols rely on the RNase-mediated hydrolysis of probe compounds;[36,37] these hydrolysis reactions are expected to also be catalyzed by minerals in our study. As an alternative approach to differentiate mineral-catalyzed hydrolysis from hydrolysis due to possible RNase activity, we instead compared the expected products from abiotic and enzymatic hydrolysis reactions as detailed below.

Incubation and Extraction Procedures. During the incubation phase in a standard experiment (Figure 1A), 23.3 ng/μL nucleic acid was adsorbed to goethite in 60 μL of buffer at pH 7 containing 10 mM sodium chloride (NaCl) and 3 mM 3-(4-morpholino)propane sulfonic acid (MOPS). In further experiments involving goethite, the incubation buffer was modified to alter pH, ionic strength, and composition, as indicated in figures and their captions. Further changes to the buffer were made in additional experiments involving minerals other than goethite (i.e., silica, hematite, montmorillonite, kaolinite, gibbsite, and aluminum oxide). These buffer modifications are also listed in the corresponding figures and their captions. In addition, for silica and aluminum oxide, the overall sample volume was increased to 100 μL but was maintained at 60 μL for other minerals as was used for goethite. For each combination of nucleic acid, mineral, and buffer, the mineral loadings were selected so that nucleic acids were present at 70% of their estimated adsorption capacity for specific mineral and solution conditions (Section S4). This value was selected so that nucleic acids were primarily adsorbed to minerals rather than in solution.[35,38]

Samples were agitated using a Thermomixer at 800 rpm and 25 °C for the duration of the incubation period and then centrifuged (21,100 g, 5 min) before the solution was exchanged with the extraction buffer to liberate adsorbed nucleic acids (Figure 1A). The volume of extraction buffer was selected to maintain a constant solution volume as that used during incubation (Section S5). The extraction buffer (pH 7, 3 mM MOPS, 100 mM sodium chloride, and 12 mM orthophosphate) was adapted from a previously developed buffer.[31,35] Like the prior buffer, this buffer included orthophosphate to compete with nucleic acids for binding sites.[31,35] However, the buffer pH value was decreased from highly alkaline to neutral (matching the value used during incubation) to avoid potential pH-dependent effects on hydrolysis occurring during the extraction step. In addition, the ionic strength was increased by adding sodium chloride to

https://doi.org/10.1021/acs.est.3c01407
Environ. Sci. Technol. 2023, 57, 8280−8288

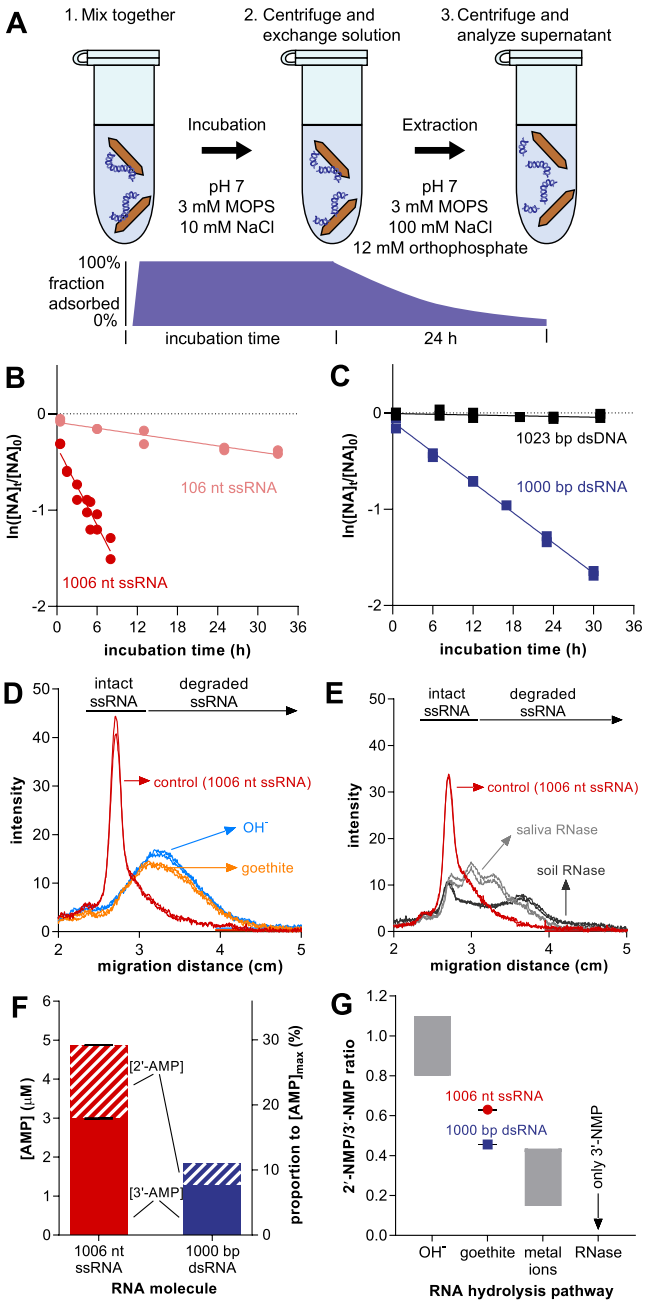

Figure 1. Hydrolysis of RNA adsorbed to goethite. (A) Schematic of the experimental approach depicting the fraction of nucleic acids in the adsorbed state at each stage. (B,C) Loss of intact ssRNA, dsRNA, and dsDNA adsorbed to goethite. (D,E) Intensity plots of control ssRNA (1006 nt) and ssRNA hydrolyzed by goethite, OH^- (i.e. alkaline pH), saliva RNase, and soil RNase to comparable degradation extents (Figure S11). (F) Generation of adenosine monophosphate (AMP) from goethite-catalyzed RNA hydrolysis after 190 d of incubation. $[AMP]_{max}$ denotes the AMP concentration if RNA molecules were fully hydrolyzed to nucleoside monophosphate (NMP), which was simplified for presentation as a single value (16.3 μM) that is the average of marginally different values for ssRNA (16.7 μM) and dsRNA (15.9 μM). The concentrations of 3′-AMP from dsRNA in duplicate samples were identical at the instrumental precision level. Samples are prepared in duplicate in (B–F). Error bars represent the range of results. (G) Ratios of 3′-NMP/2′-NMP generated from hydrolysis of RNA catalyzed by OH^- (i.e., alkaline pH),[25,45] goethite (this study), metal ions,[29] and RNase,[46] as detailed in Table S6.

reduce potential goethite-catalyzed RNA hydrolysis based on initial trials. We determined extraction periods of 24 h were required to consistently obtain recoveries greater than 70% (Figures S5 and S6). The impact of the long extraction period on our results is discussed below. The recovery was consistent across incubation times, nucleic acid types, and buffer compositions (Section S5). Other minerals required the use of different extraction conditions to achieve high recovery (Figure 4 and Section S5).

Analysis of Nucleic Acids and Hydrolysis Products. To quantify the aggregate concentrations of nucleic acids and hydrolysis products (i.e., for recovery estimates) in supernatants, we measured ultraviolet (UV) light absorbance – primarily contributed by nucleobases uninvolved in hydrolysis – using a NanoDrop One^c spectrophotometer (Thermo Fisher Scientific) (Section S6). Total concentrations of DNA, dsRNA, and ssRNA were estimated from UV absorbance at 260 nm using extinction coefficients of 0.0216, 0.0214, and 0.0266 $(ng/\mu L)^{-1}$ cm^{-1}, respectively.[39] Absorbance measurements were corrected using corresponding buffers and supernatants prepared without nucleic acids.

We measured loss of intact nucleic acids due to hydrolysis using agarose gel electrophoresis with image analysis using a prior validated protocol.[25] Briefly, this method quantifies the image intensity in a rectangular region defined by the location of nucleic acid standards within the gel. By comparing to ladders containing nucleic acid fragments of known sizes, we previously determined that the length of nucleic acids must decrease by ~25% in order to migrate outside of this region.[25] Consequently, hydrolysis detected by this method is associated with reactions that lead to substantial changes in nucleic acid length (e.g., hydrolysis toward the middle of the sequences rather than the end).

The concentrations of monomeric hydrolysis products (i.e., adenosine monophosphate, AMP) were determined using high-performance liquid chromatography (HPLC) with UV detection using a previously reported method.[25]

RESULTS AND DISCUSSION

Hydrolysis of RNA at the Goethite–Water Interface. In solutions with circumneutral pH values, adsorption of nucleic acids to goethite is strongly favored due to electrostatic attraction between negatively charged nucleic acids and net positively charged goethite (point of zero charge = 9.1, Table S2), as well as coordination between phosphate groups in nucleic acids and iron atoms on the goethite surface.[38,40,41] As polymers, nucleic acid adsorption is further favored due to their interaction with the surface at multiple binding sites.[42] These factors contribute to near-complete adsorption of nucleic acids to unsaturated goethite surfaces within minutes of mixing.[35] However, the strong adsorption of nucleic acids to goethite surfaces challenges extraction prior to the analysis of nucleic acids and their hydrolysis products. Specifically, to ensure sufficient recovery for reliable analysis, extraction of nucleic acids must be carried out over multiple hours (Figures S5 and S6),[35] which is long relative to timescales for the incubation period. During extraction, a fraction of nucleic acids remains adsorbed and continues to hydrolyze (Figures 1A and S5). Across all experiments, we held the duration of the extraction period constant, resulting in a consistent increase in hydrolysis extent across samples under equivalent experimental conditions. The amount of additional RNA hydrolyzed during extraction is reflected by a non-zero intercept visible in the

https://doi.org/10.1021/acs.est.3c01407
Environ. Sci. Technol. 2023, 57, 8280–8288

kinetic data (e.g., Figure 1B). The consistency of the amount of RNA hydrolyzed during extraction across incubation times likely resulted from intact RNA desorbing from goethite at comparable rates throughout the experiment.

At increasing incubation time, we observed decreasing concentrations of recovered intact ssRNA in the extract. Consistent with kinetics for base-catalyzed hydrolysis,[25] the amount of intact ssRNA decreases following apparent first-order kinetics (Figure 1B). The dependency of the rate on the ssRNA length was also consistent between the base-[25] and goethite-catalyzed hydrolysis: specifically, increasing the length of the initial molecule by 10-fold resulted in a proportional increase in rate constants for each pathway (i.e., 0.010(±0.001) and 0.14(±0.01) h^{-1} for 106 and 1006 nucleotide (nt) ssRNA, respectively; Figures 1B and S10). In either case, the half-lives for goethite-catalyzed hydrolysis (i.e., 70 and 5 h for 106 and 1006 nt ssRNA, respectively) were far shorter than the timescales required for ssRNA to degrade abiotically in the absence of goethite. For example, RNA remained intact for multiple months or longer without goethite under similar physicochemical conditions (i.e., neutral pH, 24 °C).[25] Notably, the half-lives for goethite-catalyzed hydrolysis are comparable to timescales for dissipation of RNA in soils and sediments.[25,30,43,44]

Beyond ssRNA, adsorption at the goethite−water interface also promoted hydrolysis of dsRNA, but not double-stranded DNA (dsDNA) (Figure 1C). The apparent first-order rate constant for dsRNA hydrolysis (i.e., 0.052(±0.001) h^{-1}) was ∼3-fold slower (Figure S10) than for ssRNA of a comparable length and sequence (Section S2). The duplex structure of dsRNA is known to impede abiotic hydrolysis catalyzed by bases or metal ions.[25,27] Notably, rates for the hydrolysis for dsRNA, if detected at all, by these solution-phase reactions were at least one magnitude slower than those for ssRNA, prohibiting these abiotic reactions from contributing significantly to dsRNA degradation in the environment. In contrast, while the hydrolysis of dsRNA at the goethite−water interface was slower than ssRNA, the half-life of the reaction (13 h) remained within the timescales for RNA dissipation in the environment, indicating that mineral-catalyzed hydrolysis may be uniquely capable of degrading dsRNA as well as ssRNA.

Unlike dsRNA, dsDNA did not undergo measurable hydrolysis at the goethite−water interface (Figure 1C). We hypothesize that this difference may result from the fact that DNA lacks the 2′-hydroxyl group found in RNA, which facilitates hydrolysis.[26] Consequently, although both nucleic acids adsorb strongly to the goethite−water interface,[38] mineral-catalyzed hydrolysis is likely to lead to the rapid and selective degradation of RNA molecules over DNA.

To support our hypothesis that the hydrolysis of RNA adsorbed to goethite occurred via an abiotic process (i.e., as opposed to degradation by RNase introduced with the goethite), we compared the products of RNA hydrolysis to other known abiotic and biotic hydrolysis pathways. Both intermediate products (i.e., shorter molecules) and ultimate products (i.e., mononucleotides) differ when generated by abiotic or biotic hydrolysis of RNA. Specifically, abiotic hydrolysis results in relatively nonselective product distributions, whereas enzymes involved in biotic reactions preferentially generate certain products.

To compare intermediate products, we plotted the intensity of a gel image as a function of the migration distance beyond the original ssRNA.[31] Shorter ssRNA molecules generated by abiotic alkaline hydrolysis fell along a smooth distribution of lengths with no discernable specific peaks (Figure 1D), consistent also with products from abiotic metal ion-catalyzed hydrolysis.[27] In contrast, enzymes from representative sources (i.e., human saliva, soil) each generate multiple specific peaks due to preferential scission of specific sequences (Figure 1E). The smooth product distribution observed for RNA products extracted from goethite (Figure 1D) is therefore suggestive of an abiotic hydrolysis pathway.

Nucleoside monophosphates (NMP) (i.e., adenosine monophosphate (AMP)) generated from RNA hydrolyzed at the goethite−water interface were also consistent with abiotic hydrolysis (Figure 1F). Because NMP generation is a slow process requiring numerous phosphodiester bonds to be cleaved, both ssRNA and dsRNA were incubated at the goethite−water interface for longer durations than the above experiments (Figure 1B−E). After 190 d of incubation, 4.87(±0.02) μM total AMP was extracted from the goethite, corresponding to ∼30% of the AMP added as ssRNA (Figure 1F). Less AMP (1.85(±0.00) μM) was recovered from dsRNA, consistent with slower hydrolysis rates. The AMP isomers were generated at 2′-AMP:3′-AMP ratios of 0.63:1 from ssRNA and 0.46:1 from dsRNA. The lower ratio from dsRNA may result from additional steric constraints associated with its duplex structure. Both ratios are intermediate between previously reported isomer product ratios for abiotic hydrolysis catalyzed by alkaline pH (0.8−1.1:1, indicating a near-random distribution)[25,45] and metal ions (0.1−0.4:1)[27,29] (Figure 1G). In comparison, enzymatic hydrolysis exclusively generates the 3′-AMP product,[46] which is inconsistent with the ratio of isomers recovered from goethite.

Solution Conditions Influence RNA Hydrolysis. The effect of solution chemistry, i.e., pH, ionic strength, and presence of competitive adsorbates, on RNA hydrolysis at the goethite−water interface was evaluated for mechanistic insight, as well as to elucidate factors that may influence the reaction in the environment. Changes to the solution chemistry were made exclusively during the incubation period, while extraction conditions remained constant (Figure 1A). For each pH and ionic strength condition, goethite loading was adjusted to keep RNA near-completely in the adsorbed state by maintaining RNA at 70% of the measured solution-specific adsorption capacity (Section S4).

Both ssRNA and dsRNA hydrolyzed to the greatest extent when the solution pH was pH 7 rather than either pH 5 or 9 (Figure 2A). Decreased hydrolysis at lower pH may indicate the involvement of hydroxide in the reaction, while decreased hydrolysis at higher pH resulted from less contact between the RNA and goethite. Although goethite loads were increased at pH 9 to ensure RNA was almost exclusively adsorbed, adsorbed RNA molecules may adopt a conformation at the goethite−water interface that has fewer binding sites, thereby slowing the reaction. In addition, looser binding at high pH during incubation may have resulted in faster release of RNA molecules during extraction despite the use of a neutral pH buffer during the extraction step. Across all pH values, RNA hydrolysis was measurable, suggesting the broad relevance of this reaction at environmentally relevant pH values.

Hydrolysis of ssRNA and dsRNA at the goethite−water interface also occurred across solutions prepared at different ionic strengths (Figure 2B). For both RNA types, elevated ionic strength decreased the extent of hydrolysis. Increasing ionic strength leads to charge screening among the negatively

https://doi.org/10.1021/acs.est.3c01407
Environ. Sci. Technol. 2023, 57, 8280−8288

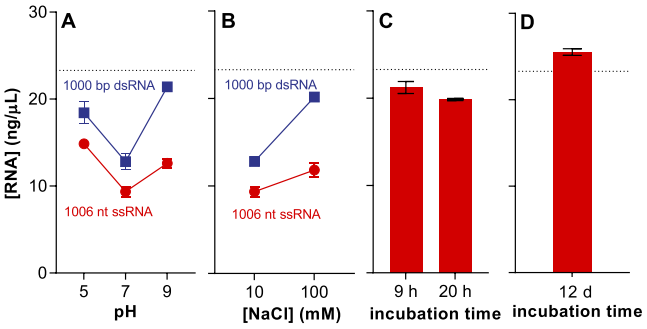

Figure 2. Intact RNA recovered from goethite incubated with varying solution chemistry. (A) pH of the adsorption solution was varied from a value of 7 (3-(4-morpholino)propane sulfonic acid, MOPS) to 5 (acetate) or 9 (tetraborate) with each buffer at 3 mM including 10 mM sodium chloride. (B) Ionic strength was increased using sodium chloride in solution held at pH 7 with 3 mM MOPS. In (A,B), incubation periods were 2 h (ssRNA) or 10 h (dsRNA), while extraction conditions were maintained constant as depicted in Figure 1A. (C,D) Goethite was pre-incubated with 0.207 μg-C/μL organic matter (Figure S12) or 12 mM orthophosphate, followed by RNA (1006 nt) addition (Section S4); RNA in the supernatant was analyzed. Error bars represent the range of measurements from duplicate samples. The dashed line refers to nominal initial RNA concentration.

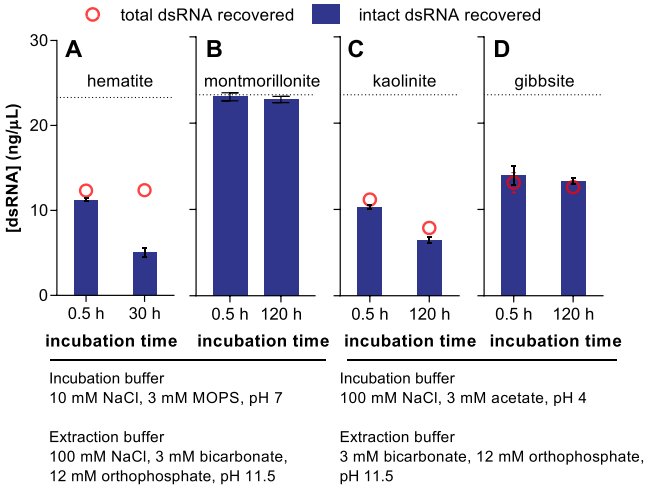

Figure 3. Intact RNA relative to total RNA (i.e., including hydrolyzed products) recovered from hematite (A), montmorillonite (B), kaolinite (C), and gibbsite (D) after incubation and extraction using specified buffers. Intact RNA recovered was determined by agarose gel electrophoresis. Total RNA recovered was determined by UV absorbance at 260 nm, except for montmorillonite due to dissolved constituents that interfered with solution absorbance. Error bars represent the range of measurements from duplicate samples. The dashed line refers to the nominal initial RNA concentration.

charged phosphodiester groups, resulting in RNA adopting a more compact conformation with fewer sites of contact with the goethite surface for each RNA molecule which may slow hydrolysis.[38]

The inclusion of soil-relevant solution constituents (i.e., organic matter, OM; orthophosphate) that compete with RNA for adsorption sites[38] confirmed the importance of contact between RNA and goethite. After goethite was pre-incubated with OM or orthophosphate sufficient to block adsorption sites (Section S4), RNA no longer measurably adsorbed to goethite, so we instead measured intact RNA concentration in solution. When incubated with OM-coated goethite, dissolved ssRNA concentrations only marginally declined (~15% over 20 h, Figure 2C). The minimal loss of ssRNA may result from degradation (e.g., by abiotic or enzymatic constituents introduced with the OM) or slow adsorption (e.g., to goethite upon replacement of OM or to the OM itself). The inclusion of orthophosphate had an even more pronounced effect on ssRNA stability in the solution phase (Figure 2D). No loss was measured over 12 d, possibly due to fewer contaminants introduced with the orthophosphate than OM or more complete and irreversible blocking of sorption sites on the goethite surface. Consequently, catalyzed hydrolysis of RNA in the presence of goethite appears to specifically require adsorption of RNA at the mineral-water interface.

RNA Hydrolysis Catalyzed by Other Minerals. We next evaluated the capacity of minerals beyond goethite to catalyze RNA hydrolysis. Among the six additional minerals tested, silica (SiO_2) neither adsorbed nor hydrolyzed RNA (Section S5) and so was not investigated further. The other five minerals, including the iron oxide hematite (α-Fe_2O_3), the aluminum (oxyhydr)oxides gibbsite (γ-$Al(OH)_3$) and aluminum oxide (Al_2O_3), and the clays montmorillonite and kaolinite, all adsorbed RNA (Section S4). To improve RNA recovery from these diverse minerals, the pH of the extraction buffer was increased to 11.5 (Figure 3), which necessitated the use of dsRNA instead of ssRNA to avoid alkaline hydrolysis.[25]

After 0.5 h of incubation, 48(±1) and 99(±2)% of intact dsRNA were recovered from hematite and montmorillonite, respectively (Figure 3A,B). After 30 h, the recovery of total RNA (i.e., including hydrolyzed products contributing to light absorbance at 260 nm) from hematite remained similar (i.e., 53(±1)%), but the amount of intact dsRNA decreased to 22(±2)% of the added amount. The lower amount of intact dsRNA relative to total RNA indicated that hematite, an iron-containing mineral like goethite, also catalyzed RNA hydrolysis. In contrast, the recovery of intact dsRNA from montmorillonite remained complete (i.e., 97(±2)%) even after 120 h. Montmorillonite may be unable to catalyze RNA hydrolysis because RNA adsorption is limited to electrostatic interactions,[47,48] whereas iron (oxyhydr)oxides also coordinate phosphate groups in RNA.[38,40−42]

The remaining minerals strongly adsorbed dsRNA and did not permit extraction even using the alkaline buffer (Section S5). Further modification of the incubation buffer allowed dsRNA extraction from kaolinite and gibbsite, but not aluminum oxide, which was excluded from further study (Section S5). The required changes to the incubation buffer to allow dsRNA extraction (lower pH, high ionic strength) also disfavor RNA hydrolysis on goethite (Figure 2), likely corresponding to looser binding between the RNA and the mineral in both cases. Close agreement between the recoveries (ranging from 34 to 56%) of total and intact RNA after 120 h in each case suggests that RNA did not hydrolyze when adsorbed to either kaolinite or gibbsite under these conditions. Although, like goethite, these minerals may coordinate phosphate groups, phosphate that readily desorbs is instead bound via weaker electrostatic attraction[47,48] that may not facilitate RNA hydrolysis. While the nonrecoverable fraction of adsorbed RNA may undergo coordination and therefore hydrolyze, the relevance of RNA degradation by these minerals is likely limited due to its irreversible adsorption under most conditions relevant to the environment.

https://doi.org/10.1021/acs.est.3c01407
Environ. Sci. Technol. 2023, 57, 8280−8288

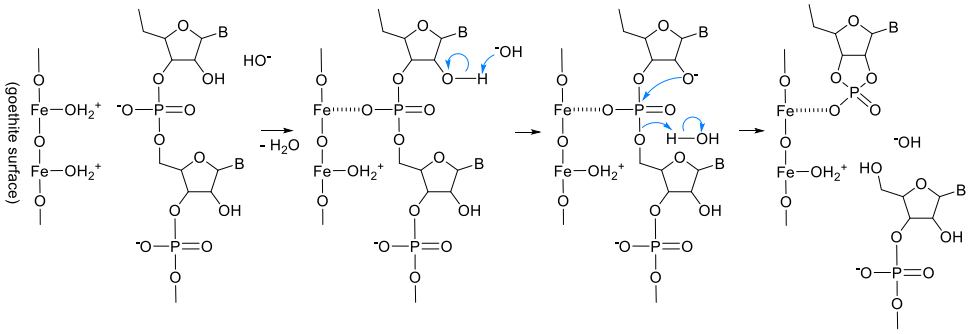

Figure 4. Proposed mechanism of catalyzed RNA hydrolysis on the surface of iron (oxyhydr)oxides (e.g., goethite). Upon RNA adsorption, both the coordination of iron with the phosphate group and the deprotonation of 2′-hydroxyl promote the nucleophilic attack on phosphorus atom, leading to the cleavage of the phosphodiester bond.

Proposed Mechanism of Mineral-Catalyzed RNA Hydrolysis. From our results, we propose that hydrolysis of mineral-adsorbed RNA is enabled by the coordination between iron atoms in iron (oxyhydr)oxides and phosphate groups in RNA (Figure 4). The lack of RNA hydrolysis when adsorption was prevented by competitors (i.e., organic matter, orthophosphate) (Figure 2C,D) supports surface-bound RNA as the primary fraction undergoing hydrolysis in the presence of iron (oxyhydr)oxides. Hydrolysis occurred when RNA was adsorbed to iron (oxyhydr)oxides like goethite known to bind nucleic acids by coordination between surface iron atoms and phosphate groups,[38,40−42] but not when RNA was adsorbed to montmorillonite (Figure 3B), which binds nucleic acids exclusively by electrostatic interactions.[48] Coordination of phosphate groups to surface metal atoms may facilitate RNA hydrolysis by drawing electron density away from the phosphorous atom, thereby increasing its electrophilicity. Dissolved metal ions that act as Lewis acids (e.g., Pb^{2+}, Zn^{2+}) are known to catalyze dissolved RNA via an analogous solution-phase mechanism.[29,49] Similar mechanisms have also been invoked to explain the hydrolysis of small organic compounds containing phosphoester bonds on mineral surfaces.[50−57] Like iron, aluminum atoms also form coordination bonds with phosphate groups;[48] however, phosphate groups bound via coordination do not desorb readily from gibbsite and kaolinite,[48] which may explain why RNA extracted from these minerals did not exhibit hydrolysis (Figure 3C,D).

While metal coordination is sufficient to catalyze hydrolysis of certain organic compounds containing phosphoester bonds,[50−57] the specificity of goethite-catalyzed hydrolysis for RNA relative to DNA (Figure 1C) indicates the additional involvement of the 2′-hydroxyl group that is present in RNA but absent in DNA. Deprotonation of the 2′-hydroxyl group forms an oxyanion, which is a strong nucleophile that subsequently attacks the phosphorous atom,[26] leading to cleavage of the phosphodiester bond (Figure 4). The intramolecular nucleophilic attack of the 2′-oxyanion is well-established to contribute to rapid hydrolysis of dissolved RNA in alkaline conditions,[26] although it is impeded in duplex molecules,[25] which may contribute to slower hydrolysis of dsRNA relative to ssRNA on goethite surfaces (Figure 1B,C). Support for the involvement of 2′-oxyanion in mineral-catalyzed hydrolysis is also provided by decreased hydrolysis of RNA at acidic pH values relative to neutral conditions (Figure 2A). The ultimate monomeric products of mineral-catalyzed RNA hydrolysis are generated at an isomeric ratio (i.e., [2′-NMP]/[3′-NMP]) that falls between ratios generated by RNA hydrolysis catalyzed by alkaline conditions (which favor the 2′-oxyanion) and dissolved metal ions (which increase the electrophilicity of the phosphorous atom) (Figure 1G), consistent with both factors contributing to RNA hydrolysis on the mineral surface.

Environmental Implications. The hydrolysis of RNA adsorbed onto iron (oxyhydr)oxides is the first abiotic hydrolysis pathway demonstrated to contribute to RNA degradation on relevant timescales (e.g., days) at environmentally relevant conditions. Furthermore, because the rapid adsorption of RNA to these minerals likely protects RNA from enzymatic degradation,[22] mineral-catalyzed hydrolysis is potentially the most important degradation pathway for adsorbed RNA, which accounts for a large fraction of RNA in soils and sediments.[31] This fate process may be particularly important in iron oxide-rich soils like Utisols, which account for approximately one-tenth of globally ice-free land.[58]

The potential for mineral-catalyzed hydrolysis to contribute to selective degradation of RNA relative to DNA must be considered when applying nucleic acid quantification in soils and sediments to ecological analysis. For example, extracted RNA may be biased lower relative to DNA when comparing transcriptomic to genomic data[1,16] and RNA to DNA viral abundances (e.g., when performing wastewater-based epidemiology).[18,19] The hydrolysis of adsorbed RNA may also limit the environmental persistence of noncoding RNA serving for natural inter-species interactions[20,21] and as engineered biopesticides in agriculture.[22,23] In all of these applications, adsorbed RNA must be returned to the solution phase to be either quantified or bioavailable. Consequently, the degradation of extractable RNA adsorbed to minerals like iron (oxyhydr)oxides that catalyze hydrolysis may be particularly relevant in comparison to nonextractable RNA that is strongly bound to aluminum (oxyhydr)oxides. While mineral-catalyzed hydrolysis of RNA ultimately generates short products (e.g., NMPs, Figure 1F) that will not be detected in these analyses, some hydrolysis products are expected to remain detectable if the site of phosphodiester bond cleavage does not overlap with the region of the RNA sequence used for detection. Faster loss rates may therefore be seen for analyses that utilize longer RNA sequences that contain more bonds at which cleavage can occur, as previously observed for nucleic acids undergoing other chemical modifications (e.g., photolysis).[59]

The hydrolysis of adsorbed RNA may also be important for biogeochemical processes (i.e., phosphorous cycling), particularly due to greater releases of RNA relative to DNA upon cell death.[1] Both DNA and RNA are phosphorous-rich biomole-

https://doi.org/10.1021/acs.est.3c01407
Environ. Sci. Technol. 2023, 57, 8280−8288

cules that serve as major pools of organic phosphorus in some environmental systems (e.g., deep-sea top sediments).[6] Mineral-catalyzed hydrolysis of adsorbed RNA may return organic phosphorous to solution by converting RNA polymers to hydrolysis products that are more weakly bound to the mineral surface.[42] Hydrolysis products may also be released upon iron reduction, thereby contributing to phosphorous cycling in fluctuating redox environments (e.g., forest soils, agricultural soils, estuarine sediments).[60−62]

■ ASSOCIATED CONTENT

Supporting Information

The Supporting Information is available free of charge at https://pubs.acs.org/doi/10.1021/acs.est.3c01407.

Sources of chemicals and molecular biology kits; sequence information; mineral synthesis, pretreatment, and characterization; determination of incubation and extraction conditions; evaluation of RNA measurements using solution absorbance; and supplementary results (PDF)

■ AUTHOR INFORMATION

Corresponding Author

Kimberly M. Parker − *Department of Energy, Environmental & Chemical Engineering, Washington University in St. Louis, St. Louis, Missouri 63130, United States;* orcid.org/0000-0002-5380-8893; Email: kmparker@wustl.edu

Authors

Ke Zhang − *Department of Energy, Environmental & Chemical Engineering, Washington University in St. Louis, St. Louis, Missouri 63130, United States;* Present Address: Department of Civil and Environmental Engineering, University of Michigan, Ann Arbor, Michigan 48109, United States (K.Z.); orcid.org/0000-0001-6407-8016

Kun-Pu Ho − *Department of Energy, Environmental & Chemical Engineering, Washington University in St. Louis, St. Louis, Missouri 63130, United States*

Anamika Chatterjee − *Department of Energy, Environmental & Chemical Engineering, Washington University in St. Louis, St. Louis, Missouri 63130, United States*

Grace Park − *Department of Energy, Environmental & Chemical Engineering, Washington University in St. Louis, St. Louis, Missouri 63130, United States*

Zhiyao Li − *Department of Energy, Environmental & Chemical Engineering, Washington University in St. Louis, St. Louis, Missouri 63130, United States*

Jeffrey G. Catalano − *Department of Earth & Planetary Sciences, Washington University in St. Louis, St. Louis, Missouri 63130, United States;* orcid.org/0000-0001-9311-977X

Complete contact information is available at: https://pubs.acs.org/10.1021/acs.est.3c01407

Notes

The authors declare no competing financial interest.

■ ACKNOWLEDGMENTS

This work is supported by the USDA Biotechnology Risk Assessment Grant Program Award 2017-33522-26998 (K.M.P.), NSF CAREER Award 2046602 (K.M.P.), American Chemical Society − Petroleum Research Fund 60057-DNI4 (K.M.P.), and the NASA Astrobiology Program Award No. 80NSSC19M0069 (J.G.C.). We thank Yao Ma and Daniel Giammar for determining the crystal structure of synthesized minerals. We thank Fuzhong Zhang for access to the gel image system.

■ REFERENCES

(1) Torti, A.; Lever, M. A.; Jørgensen, B. B. Origin, dynamics, and implications of extracellular DNA pools in marine sediments. *Mar. Genomics* **2015**, *24*, 185−196.

(2) Carini, P.; Marsden, P. J.; Leff, J. W.; Morgan, E. E.; Strickland, M. S.; Fierer, N. Relic DNA is abundant in soil and obscures estimates of soil microbial diversity. *Nat. Microbiol.* **2017**, *2*, 16242.

(3) Mauvisseau, Q.; Harper, L. R.; Sander, M.; Hanner, R. H.; Kleyer, H.; Deiner, K. The Multiple States of Environmental DNA and What Is Known about Their Persistence in Aquatic Environments. *Environ. Sci. Technol.* **2022**, *56*, 5322−5333.

(4) Mao, D.; Luo, Y.; Mathieu, J.; Wang, Q.; Feng, L.; Mu, Q.; Feng, C.; Alvarez, P. J. J. Persistence of Extracellular DNA in River Sediment Facilitates Antibiotic Resistance Gene Propagation. *Environ. Sci. Technol.* **2014**, *48*, 71−78.

(5) Grunenwald, A.; Keyser, C.; Sautereau, A. M.; Crubézy, E.; Ludes, B.; Drouet, C. Adsorption of DNA on biomimetic apatites: Toward the understanding of the role of bone and tooth mineral on the preservation of ancient DNA. *Appl. Surf. Sci.* **2014**, *292*, 867−875.

(6) Dell'Anno, A.; Danovaro, R. Extracellular DNA Plays a Key Role in Deep-Sea Ecosystem Functioning. *Science* **2005**, *309*, 2179−2179.

(7) Blum, S. A. E.; Lorenz, M. G.; Wackernagel, W. Mechanism of Retarded DNA Degradation and Prokaryotic Origin of DNases in Nonsterile Soils. *Syst. Appl. Microbiol.* **1997**, *20*, 513−521.

(8) Aardema, B. W.; Lorenz, M. G.; Krumbein, W. E. Protection of Sediment-Adsorbed Transforming DNA Against Enzymatic Inactivation. *Appl. Environ. Microbiol.* **1983**, *46*, 417−420.

(9) Lorenz, M. G.; Wackernagel, W. Adsorption of DNA to sand and variable degradation rates of adsorbed DNA. *Appl. Environ. Microbiol.* **1987**, *53*, 2948−2952.

(10) Romanowski, G.; Lorenz, M. G.; Wackernagel, W. Adsorption of plasmid DNA to mineral surfaces and protection against DNase I. *Appl. Environ. Microbiol.* **1991**, *57*, 1057−1061.

(11) Paget, E.; Monrozier, L. J.; Simonet, P. Adsorption of DNA on clay minerals: protection against DNaseI and influence on gene transfer. *FEMS Microbiol. Lett.* **1992**, *97*, 31−39.

(12) Khanna, M.; Stotzky, G. Transformation of *Bacillus subtilis* by DNA bound on montmorillonite and effect of DNase on the transforming ability of bound DNA. *Appl. Environ. Microbiol.* **1992**, *58*, 1930−1939.

(13) Lorenz, M. G.; Wackernagel, W. Bacterial gene transfer by natural genetic transformation in the environment. *Microbiol. Rev.* **1994**, *58*, 563−602.

(14) Cai, P.; Huang, Q. Y.; Zhang, X. W. Interactions of DNA with Clay Minerals and Soil Colloidal Particles and Protection against Degradation by DNase. *Environ. Sci. Technol.* **2006**, *40*, 2971−2976.

(15) Stotzky, G. Persistence and Biological Activity in Soil of Insecticidal Proteins from *Bacillus thuringiensis* and of Bacterial DNA Bound on Clays and Humic Acids. *J. Environ. Qual.* **2000**, *29*, 691−705.

(16) Yates, M. C.; Derry, A. M.; Cristescu, M. E. Environmental RNA: A Revolution in Ecological Resolution? *Trends Ecol. Evol.* **2021**, *36*, 601−609.

(17) Larsen, D. A.; Wigginton, K. R. Tracking COVID-19 with wastewater. *Nat. Biotechnol.* **2020**, *38*, 1151−1153.

(18) Silverman, A. I.; Boehm, A. B. Systematic Review and Meta-Analysis of the Persistence and Disinfection of Human Coronaviruses and Their Viral Surrogates in Water and Wastewater. *Environ. Sci. Technol. Lett.* **2020**, *7*, 544−553.

(19) Silverman, A. I.; Boehm, A. B. Systematic Review and Meta-Analysis of the Persistence of Enveloped Viruses in Environmental

Waters and Wastewater in the Absence of Disinfectants. *Environ. Sci. Technol.* **2021**, *55*, 14480−14493.
(20) de Bruijn, I.; Verhoeven, K. J. F. Cross-species interference of gene expression. *Nat. Commun.* **2018**, *9*, 5019.
(21) Huang, C. Y.; Wang, H.; Hu, P.; Hamby, R.; Jin, H. Small RNAs − Big Players in Plant-Microbe Interactions. *Cell Host Microbe* **2019**, *26*, 173−182.
(22) Mitter, N.; Worrall, E. A.; Robinson, K. E.; Li, P.; Jain, R. G.; Taochy, C.; Fletcher, S. J.; Carroll, B. J.; Lu, G. Q.; Xu, Z. P. Clay nanosheets for topical delivery of RNAi for sustained protection against plant viruses. *Nat. Plants* **2017**, *3*, 16207.
(23) Baum, J. A.; Bogaert, T.; Clinton, W.; Heck, G. R.; Feldmann, P.; Ilagan, O.; Johnson, S.; Plaetinck, G.; Munyikwa, T.; Pleau, M.; Vaughn, T.; Roberts, J. Control of coleopteran insect pests through RNA interference. *Nat. Biotechnol.* **2007**, *25*, 1322−1326.
(24) Parker, K. M.; Sander, M. Environmental Fate of Insecticidal Plant-Incorporated Protectants from Genetically Modified Crops: Knowledge Gaps and Research Opportunities. *Environ. Sci. Technol.* **2017**, *51*, 12049−12057.
(25) Zhang, K.; Hodge, J.; Chatterjee, A.; Moon, T. S.; Parker, K. M. Duplex Structure of Double-Stranded RNA Provides Stability against Hydrolysis Relative to Single-Stranded RNA. *Environ. Sci. Technol.* **2021**, *55*, 8045−8053.
(26) Li, Y.; Breaker, R. R. Kinetics of RNA Degradation by Specific Base Catalysis of Transesterification Involving the 2'-Hydroxyl Group. *J. Am. Chem. Soc.* **1999**, *121*, 5364−5372.
(27) Chatterjee, A.; Zhang, K.; Rao, Y.; Sharma, N.; Giammar, D. E.; Parker, K. M. Metal-Catalyzed Hydrolysis of RNA in Aqueous Environments. *Environ. Sci. Technol.* **2022**, *56*, 3564−3574.
(28) Oivanen, M.; Kuusela, S.; Lönnberg, H. Kinetics and Mechanisms for the Cleavage and Isomerization of the Phosphodiester Bonds of RNA by Brønsted Acids and Bases. *Chem. Rev.* **1998**, *98*, 961−990.
(29) Shelton, V. M.; Morrow, J. R. Catalytic transesterification and hydrolysis of RNA by zinc(II) complexes. *Inorg. Chem.* **1991**, *30*, 4295−4299.
(30) Fischer, J. R.; Zapata, F.; Dubelman, S.; Mueller, G. M.; Uffman, J. P.; Jiang, C.; Jensen, P. D.; Levine, S. L. Aquatic fate of a double-stranded RNA in a sediment−water system following an overwater application. *Environ. Toxicol. Chem.* **2017**, *36*, 727−734.
(31) Parker, K. M.; Barragán Borrero, V.; van Leeuwen, D. M.; Lever, M. A.; Mateescu, B.; Sander, M. Environmental fate of RNA interference pesticides: Adsorption and degradation of double-stranded RNA molecules in agricultural soils. *Environ. Sci. Technol.* **2019**, *53*, 3027−3036.
(32) Albright, V. C.; Wong, C. R.; Hellmich, R. L.; Coats, J. R. Dissipation of double-stranded RNA in aquatic microcosms. *Environ. Toxicol. Chem.* **2017**, *36*, 1249−1253.
(33) Miyamoto, T.; Okano, S.; Kasai, N. Irreversible thermoinactivation of ribonuclease-A by soft-hydrothermal processing. *Biotechnol. Prog.* **2009**, *25*, 1678−1685.
(34) Schwertmann, U., Relations Between Iron Oxides, Soil Color, and Soil Formation. In *Soil Color*; 1993; pp 51−69.
(35) Zhang, K.; Wei, J.; Huff Hartz, K. E.; Lydy, M. J.; Moon, T. S.; Sander, M.; Parker, K. M. Analysis of RNA Interference (RNAi) Biopesticides: Double-Stranded RNA (dsRNA) Extraction from Agricultural Soils and Quantification by RT-qPCR. *Environ. Sci. Technol.* **2020**, *54*, 4893−4902.
(36) Tong, C.; Zhao, C.; Liu, B.; Li, B.; Ai, Z.; Fan, J.; Wang, W. Sensitive Detection of RNase A Activity and Collaborative Drug Screening Based on rGO and Fluorescence Probe. *Anal. Chem.* **2018**, *90*, 2655−2661.
(37) ThermoFisher, RNaseAlert™ Lab Test Kit. Available at https://assets.thermofisher.com/TFS-Assets/LSG/manuals/fm_1964.pdf (accessed 2023-05-01).
(38) Sodnikar, K.; Parker, K. M.; Stump, S. R.; ThomasArrigo, L. K.; Sander, M. Adsorption of double-stranded ribonucleic acids (dsRNA) to iron (oxyhydr-)oxide surfaces: comparative analysis of model dsRNA molecules and deoxyribonucleic acids (DNA). *Environ. Sci.: Process. Impacts* **2021**, *23*, 605−620.
(39) Nwokeoji, A. O.; Kilby, P. M.; Portwood, D. E.; Dickman, M. J. Accurate Quantification of Nucleic Acids Using Hypochromicity Measurements in Conjunction with UV Spectrophotometry. *Anal. Chem.* **2017**, *89*, 13567−13574.
(40) Schmidt, M. P.; Martínez, C. E. Supramolecular Association Impacts Biomolecule Adsorption onto Goethite. *Environ. Sci. Technol.* **2018**, *52*, 4079−4089.
(41) Schmidt, M. P.; Martínez, C. E. Ironing Out Genes in the Environment: An Experimental Study of the DNA−Goethite Interface. *Langmuir* **2017**, *33*, 8525−8532.
(42) Holm, N. G.; Ertem, G.; Ferris, J. P. The binding and reactions of nucleotides and polynucleotides on iron oxide hydroxide polymorphs. *Origins Life Evol. Biospheres* **1993**, *23*, 195−215.
(43) Dubelman, S.; Fischer, J.; Zapata, F.; Huizinga, K.; Jiang, C.; Uffman, J.; Levine, S.; Carson, D. Environmental fate of double-stranded RNA in agricultural soils. *PLoS One* **2014**, *9*, No. e93155.
(44) Kunadiya, M. B.; Burgess, T. I.; Dunstan, W. A.; White, D.; StJ. Hardy, G. E. Persistence and degradation of *Phytophthora cinnamomi* DNA and RNA in different soil types. *Environ. DNA* **2021**, *3*, 92−104.
(45) Komiyama, M.; Takeshige, Y. Regioselective phosphorus-oxygen(3′) cleavage of 2′,3′-cyclic monophosphates of ribonucleosides catalyzed by *β*- and *γ*-cyclodextrins. *J. Org. Chem.* **1989**, *54*, 4936−4939.
(46) Dugas, H.; Penney, C., Bioorganic Chemistry of the Phosphates. In *Bioorganic Chemistry: A Chemical Approach to Enzyme Action*; Springer US, 1981; pp 93−178.
(47) Ferris, J. P.; Ertem, G.; Agarwal, V. K. The adsorption of nucleotides and polynucleotides on montmorillonite clay. *Origins Life Evol. Biospheres* **1989**, *19*, 153−164.
(48) Van Emmerik, T. J.; Sandström, D. E.; Antzutkin, O. N.; Angove, M. J.; Johnson, B. B. ^{31}P Solid-State Nuclear Magnetic Resonance Study of the Sorption of Phosphate onto Gibbsite and Kaolinite. *Langmuir* **2007**, *23*, 3205−3213.
(49) Breslow, R.; Huang, D. L. Effects of metal ions, including Mg^{2+} and lanthanides, on the cleavage of ribonucleotides and RNA model compounds. *Proc. Natl. Acad. Sci. U. S. A.* **1991**, *88*, 4080−4083.
(50) Fang, Y.; Kim, E.; Strathmann, T. J. Mineral- and Base-Catalyzed Hydrolysis of Organophosphate Flame Retardants: Potential Major Fate-Controlling Sink in Soil and Aquatic Environments. *Environ. Sci. Technol.* **2018**, *52*, 1997−2006.
(51) Torrents, A.; Stone, A. T. Oxide Surface-Catalyzed Hydrolysis of Carboxylate Esters and Phosphorothioate Esters. *Soil Sci. Soc. Am. J.* **1994**, *58*, 738−745.
(52) Mäkie, P.; Persson, P.; Österlund, L. Adsorption of trimethyl phosphate and triethyl phosphate on dry and water pre-covered hematite, maghemite, and goethite nanoparticles. *J. Colloid Interface Sci.* **2013**, *392*, 349−358.
(53) Wan, B.; Yang, P.; Jung, H.; Zhu, M.; Diaz, J. M.; Tang, Y. Iron oxides catalyze the hydrolysis of polyphosphate and precipitation of calcium phosphate minerals. *Geochim. Cosmochim. Acta* **2021**, *305*, 49−65.
(54) Xiao-Lan, H., Iron Oxide Nanoparticles: An Inorganic Phosphatase. In *Nanocatalysts*; IntechOpen, 2019; pp 97−124. DOI: 10.5772/intechopen.82650
(55) Tan, F.; Zhang, Y.; Wang, J.; Wei, J.; Cai, Y.; Qian, X. An efficient method for dephosphorylation of phosphopeptides by cerium oxide. *J. Mass Spectrom.* **2008**, *43*, 628−632.
(56) Olsson, R.; Giesler, R.; Loring, J. S.; Persson, P. Adsorption, Desorption, and Surface-Promoted Hydrolysis of Glucose-1-Phosphate in Aqueous Goethite (*α*-FeOOH) Suspensions. *Langmuir* **2010**, *26*, 18760−18770.
(57) Baldwin, D. S.; Beattie, J. K.; Coleman, L. M.; Jones, D. R. Hydrolysis of an Organophosphate Ester by Manganese Dioxide. *Environ. Sci. Technol.* **2001**, *35*, 713−716.
(58) Weil, R. R.; Brady, N. C., *The Nature and Properties of Soils*, 15th Ed.; Pearson: London, U.K., 2017.

(59) Dunn, F. B.; Silverman, A. I. Sunlight Photolysis of Extracellular and Intracellular Antibiotic Resistance Genes tetA and sul2 in Photosensitizer-Free Water. *Environ. Sci. Technol.* **2021**, *55*, 11019.
(60) Peretyazhko, T.; Sposito, G. Iron(III) reduction and phosphorous solubilization in humid tropical forest soils. *Geochim. Cosmochim. Acta* **2005**, *69*, 3643−3652.
(61) McRose, D. L.; Newman, D. K. Redox-active antibiotics enhance phosphorus bioavailability. *Science* **2021**, *371*, 1033−1037.
(62) Queiroz, H. M.; Ferreira, T. O.; Barcellos, D.; Nóbrega, G. N.; Antelo, J.; Otero, X. L.; Bernardino, A. F. From sinks to sources: The role of Fe oxyhydroxide transformations on phosphorus dynamics in estuarine soils. *J. Environ. Manage.* **2021**, *278*, No. 111575.

https://doi.org/10.1021/acs.est.3c01407
Environ. Sci. Technol. 2023, 57, 8280−8288